PAPER

Check for updates

Tetranuclear Cu(II)-chiral complexes: synthesis, characterization and biological activity†

Krisana Peewasan,*[a] Marcel P. Merkel,[b] Kristof Zarschler, [ID][c] Holger Stephan, [ID][c] Christopher E. Anson [ID][a] and Annie K. Powell [ID]*[ab]

Tetranuclear chiral Cu(II)-Schiff-base complexes **S-1** and **R-1**, were synthesised using enantiomerically pure (S)-(H$_2$vanPheol) and (R)-(H$_2$vanPheol) ligands respectively in the ratio of 1 : 1 of Cu(NO$_3$)$_2$ to (S/R)-(H$_2$vanPheol) in MeOH at room temperature. A pair of polynuclear chiral Cu(II)-cluster complexes were characterized using single-crystal X-ray diffraction, elemental analysis, infrared and CD spectroscopy. The results revealed the importance of these chiral ligands encouraging the arrangement of copper metal in non-centrosymmetric polar packing. The potential of the novel [Cu$_4$(S/R-vanPheol)$_2$(S/R-HvanPheol)$_2$(CH$_3$OH)$_2$](NO$_3$)$_2$ complexes as biologically active compounds was assessed in particular regarding their anti-proliferative and anti-microbial properties.

Introduction

Applications of metal-based drugs are of great interest, in particular to final alternatives to the Pt-based anticancer drug cisplatin.[1–4] The metals can have variable coordination number, geometry, and redox states. To date, cisplatin is one of the most widely used anticancer drugs although it shows significant side-effects such as nausea, bone-marrow production suppression, and nephrotoxicity.[1] Aiming to diminish the side effects and resistance caused by cisplatin, the development of new therapeutic metal-based treatments are needed. Requirements for the desired high efficiency therapeutic metal-based drugs are (i) high inhibition of tumour angiogenesis with simultaneous tumour cell death, (ii) diminishing the side effects and resistance caused by cisplatin and (iii) biological activity in living organisms.[5] To this end, copper is a good candidate in comparison to other transition metals because it acts as a cofactor during the angiogenesis process[6–8] where it enhances the production of cytokinase, endothelial cell proliferation and migration. The chelation of copper ions can also suppress

angiogenesis and decrease tumour volume in animals.[9–12] Recent studies reveal that the use of novel Schiff-base copper(II)-based complexes can remarkably induce apoptosis, inhibit proliferation, suppress migration, metastasis and angiogenesis and thus inhibit the growth of cervical cancer.[13–22] Schiff-base ligand derivatives have been widely used in coordination chemistry due to the advantages of their flexible properties and the easy manipulation of their coordination properties *via* the variation of functional groups such as amine, alcohol, carboxylate and sulfonate.[23–26] Out of the small number of Cu(II) complexes formed with pocket ligands only one of these employs a chiral ligand and none contain Cu(II) coordination clusters.

Herein we report the development of an ambient condition synthesis with high yields where enantioselectivity provides an atom efficient route to this system. The new enantiomerically pure ligands were selected since they provide a tetradentate coordination pocket which is ideally suited to accommodate Cu(II)-ions to give the enantiopure complexes, [Cu$_4$(S-vanPheol)$_2$(S-HvanPheol)$_2$(CH$_3$OH)$_2$](NO$_3$)$_2$ (**S-1**) and [Cu$_4$(R-vanPheol)$_2$(R-HvanPheol)$_2$(CH$_3$OH)$_2$](NO$_3$)$_2$ (**R-1**) *via* self-assembly in methanol under aerobic conditions. The single-crystal X-ray diffraction, elemental analysis, infrared and circular dichroism (CD) spectroscopy of Cu(II)-complexes and biological activities have been investigated.

Results and discussion

The synthesis of the Schiff-base ligands S/R-(H$_2$vanPheol) (Scheme 1) was performed by the condensation reaction between 2-hydroxy-3-methoxybenzaldehyde (*o*-vanillin) and enantiomerically pure S- or R-2-amino-3-phenyl-1-propanol (phenylaninol) under reflux in absolute ethanol.[27] The

[a]Institute of Inorganic Chemistry, Karlsruhe Institute of Technology, Engesserstrasse 15, 76131 Karlsruhe, Germany. E-mail: Krisana.peewasan@kit.edu; christopher. anson@kit.edu

[b]Institute of Nanotechnology, Karlsruhe Institute of Technology, Campus North, Hermann-von-Helmholtz-Platz 1, Eggenstein-Leopoldshafen, 76344, Karlsruhe, Germany. E-mail: Marcel.merkel@kit.edu; annie.powell@kit.edu

[c]Institute of Radiopharmaceutical Cancer Research, Helmholtz-ZentrumDresden-Rossendorf, D-01328 Dresden, Germany. E-mail: k.zarschler@hzdr.de; h.stephan@hzdr.de
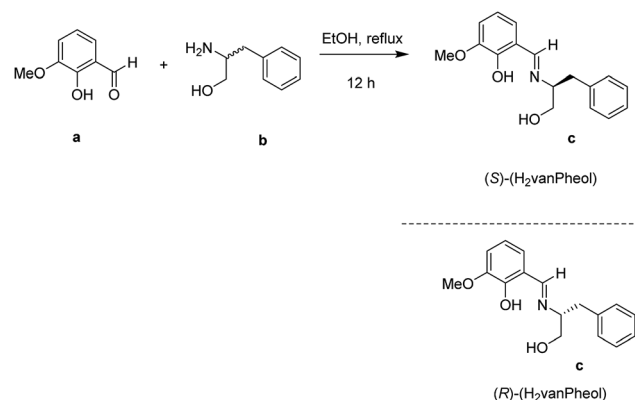
Scheme 1 Preparation of Schiff-bases (S)/(R)-(H₂vanPheol).

corresponding chiral Schiff-base ligand S-(H$_2$vanPheol) or R-(H$_2$vanPheol) was reacted with Cu(NO$_3$)$_2$ in methanol. Green block-like crystals of the complex **S-1** or **R-1** with formula [Cu$_4$(S/R-vanPheol)$_2$(S/R-HvanPheol)$_2$(CH$_3$OH)$_2$](NO$_3$)$_2$ were obtained after 7 days.

Single-crystal X-ray analysis shows that **S-1** and **R-1** are isostructural and crystallize in the polar space group $P2_1$ with $Z = 2$ (Table 1).

Crystallization in a polar space group with Flack χ parameters of zero highlights the efficient transfer of chirality from the chiral Schiff-base ligand to the coordination compound. Due to the fact that **S-1** and **R-1** are a pair of enantiomers **S-1** is selected as a representative to describe the specific structure here.

According to the X-ray crystallographic analyses, **S-1** is composed of an independent tetranuclear Cu(II) cluster combining four Schiff-base ligands, which are oriented around the cluster (Fig. 1). In each cluster, two ligands are doubly-deprotonated, with their alkoxo oxygens (O6 or O12) forming μ_3-bridges between copper centres, while the other two are singly-deprotonated, with their alkoxy O–H groups (O3 or O9) forming hydrogen bonds to nitrate counterions. In each tetranuclear Cu(II) cluster compound, the core structure can be regarding being based on a Cu$_4$O$_4$ cubane unit, in which the Cu^{2+} centres are bridged by four deprotonated oxygens from ligands. Although the two alkoxo oxygen (O6 and O12) form μ_3-bridges, the two phenoxo oxygens O2 and O8 only form μ_2-bridges. This results in a partial opening of the tetracubane core, with the Cu3⋯O2 and Cu1⋯O8 edges now both over 3.2 Å. The edges Cu1⋯Cu4 and Cu2⋯Cu3 are each further supported by a hydrogen bond between the O–H of a methanol ligand and a deprotonated but non-bridging phenoxo oxygen.

The charge balance is provided by two nitrate anions, which form intermolecular hydrogen bonds with propanol groups of the ligand. The Cu–O distances range from 1.904(4) to 2.423(4) Å, whereas the Cu–N distances are between 1.930(5) and 1.948(5) Å. In addition, the O–Cu–O angles lie between 106.9(19)° to 127.1(2)° and the N–Cu–O angles between 82.31(19)° and 172.8(2)° (Table S1†). In **R-1**, the unidentate ligand coordinating to Cu1 is not pure methanol, but a disordered superposition of methanol (70%) and water (30%). This disordered mixture influences the position of the neighbouring nitrate since through the presence of coordinated H$_2$O, the

Table 1 Crystallographic data of complexes **S-1** and **R-1**

|	S-1	R-1
Empirical formula	C$_{71}$H$_{82}$Cu$_4$N$_6$O$_{21}$	C$_{70.7}$H$_{80.8}$Cu$_4$N$_6$O$_{21}$
Formula weight	1609.58	1604.77
Temperature/K	180(2)	180.15
Crystal system	Monoclinic	Monoclinic
Space group	$P2_1$	$P2_1$
a [Å]	10.6198(7)	10.5835(8)
b [Å]	21.4213(14)	21.529(2)
c [Å]	15.6347(12)	15.5711(12)
α [°]	90	90
β [°]	94.833(6)	94.696(6)
γ [°]	90	90
Volume [Å^3]	3544.1(4)	3536.0(5)
Z	2	2
ρ_{calc} [g cm^{-3}]	1.508	1.507
μ [mm^{-1}]	1.263	1.266
$F(000)$	1668	1662
Crystal size [mm^3]	0.34 × 0.18 × 0.16	0.58 × 0.23 × 0.18
Radiation	MoKα ($\lambda = 0.71073$)	MoKα ($\lambda = 0.71073$)
2θ range for data collection [°]	3.232 to 53.462	3.784 to 52.742
Index ranges	$-13 \leq h \leq 13, -24 \leq k \leq 27, -16 \leq l \leq 19$	$-11 \leq h \leq 13, -26 \leq k \leq 26, -19 \leq l \leq 19$
Reflections collected	29 165	28 025
Independent reflections	14 517 [$R_{int} = 0.0493, R_{sigma} = 0.0652$]	14 367 [$R_{int} = 0.0873, R_{sigma} = 0.0750$]
Data/restraints/parameters	14 517/29/940	14 367/34/935
Goodness-of-fit on F^2	0.938	0.978
Final R indices [$I > 2\sigma(I)$]	0.0380	0.0431
Final wR_1 indices [all data]	0.0936	0.1200
Largest diff. peak/hole [e Å^{-3}]	0.53/−0.62	0.73/−0.63
Flack parameter	−0.010(7)	−0.003(15)

S-1

R-1
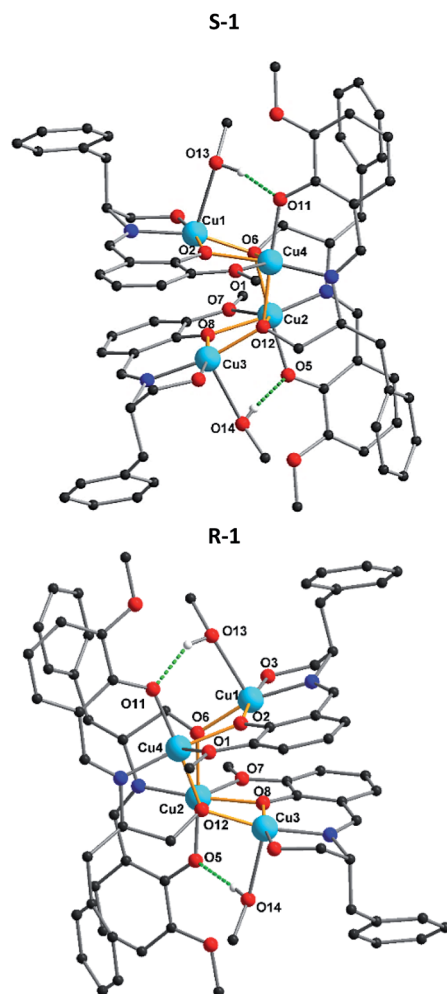
Fig. 1   The structures of **S-1** and **R-1**. The hydrogen atoms and nitrate counterions are omitted for clarity. Hydrogen bonds are shown as green dashed lines. Colour codes for the atoms: light blue (Cu), blue (N), red (O) and black (C).

Fig. 2   CD spectra of 50 μM solution of **S-1** and **R-1** in MeOH.

Crystalline samples of **S-1** and **R-1** were prepared as 50 μM solution in MeOH and their optical properties were evaluated using circular dichroism (CD). **S-1** and **R-1** display opposite Cotton effects over the measured range to give the expected mirror image spectra. **S-1** exhibits an intermediate positive peak at 247 nm and strong negative peak at 271 nm plus a broad negative peak at 371 nm. The mirror image complex **R-1**, displays absorption peaks of the opposite sign in the same wavelength range (Fig. 2).

The effect of **S-1** and **R-1** on the viability of living human cells was investigated using the two cell lines A431 and HEK293 (Fig. 3). These *in vitro* studies revealed a comparable concentration-dependent decrease in the number of metabolically active cells for both enantiomers. This suggests that the observed effects of the complexes are independent of their chirality. Interestingly, the human embryonic kidney cell line HEK293 seems to be more sensitive to exposure to **S-1** and **R-1**

nitrate is pulled closer to the core structure than in methanol case. The FTIR spectra in the region 4000–400 cm^{-1} for complexes **S-1** and **R-1** have been evaluated (Fig. S5†). The comparison of these complexes with the free ligand revealed that the strong and sharp bands in the region 1629–1630 cm^{-1} can be assigned to the azomethine ν(C=N) stretching frequency of the coordinated ligands in **S-1** and **R-1**. The shift of this band towards a lower frequency compared to that of the free ligands (1642–1605 cm^{-1}) indicates the coordination of the imine nitrogen atom to the metal centre. The broad band around 3551–3167 cm^{-1} is due to the ν(OH) of the alcohol coordinated to the metal centre. The other ν(C–H), ν(C=C) and ν(C–O) vibrations are found in the normal ranges for these types of linkages.[26] The maxima in the UV/vis absorption spectra of complexes **S-1** and **R-1** at 376 nm (π–π*) and 660 nm (n–π*), Cu(II) charge transfer transition, were found to be blue shifted from 419 nm in comparison to the free ligand. (Fig. S6†). No fluorescence emission was observed for either complex possibly as a result of the quenching effect of unoccupied d orbitals of the copper(II) through the nonradiative dissipation process.[28]
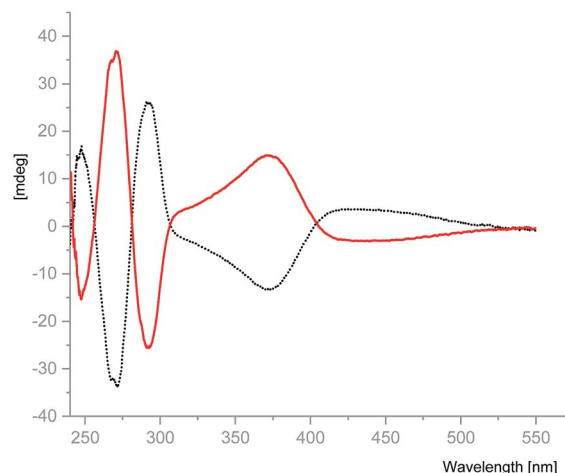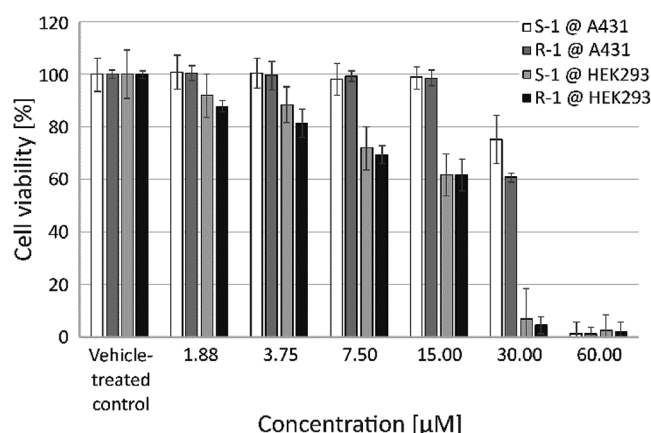

Fig. 3   *In vitro* viability evaluation of A431 and HEK293 cells after treatment with **S-1** and **R-1** for 48 h. The cellular metabolism was determined as a measure of viability using a MTS assay. The percentage of cell viability is expressed relative to vehicle-treated control cells that were treated with the corresponding concentration of DMSO (final concentration 0.4%).

Table 2 IC$_{50}$ values after incubation of A431 and HEK293 cells with S-1 and R-1 for 48 h

IC$_{50}$ [μM]	A431	HEK293
S-1	45.28 ± 10.21	13.47 ± 1.97
R-1	39.16 ± 7.95	12.10 ± 1.57
Cisplatin	7.8 ± 7.95	8.1 ± 7.95

compared to the more robust epidermoid human cancer cell line A431 (Fig. 3). Consequently, the respective IC$_{50}$ values for HEK293 are less than half the values of A431 and are in the same range as cisplatin (Table 2).

In addition to the viability assessment with regard to human cells, the antibacterial activity of both compounds was evaluated in the batch cultures, Gram-positive *B. subtilis* (Fig. 4) as well as Gram-negative *E. coli* (Fig. S7†).
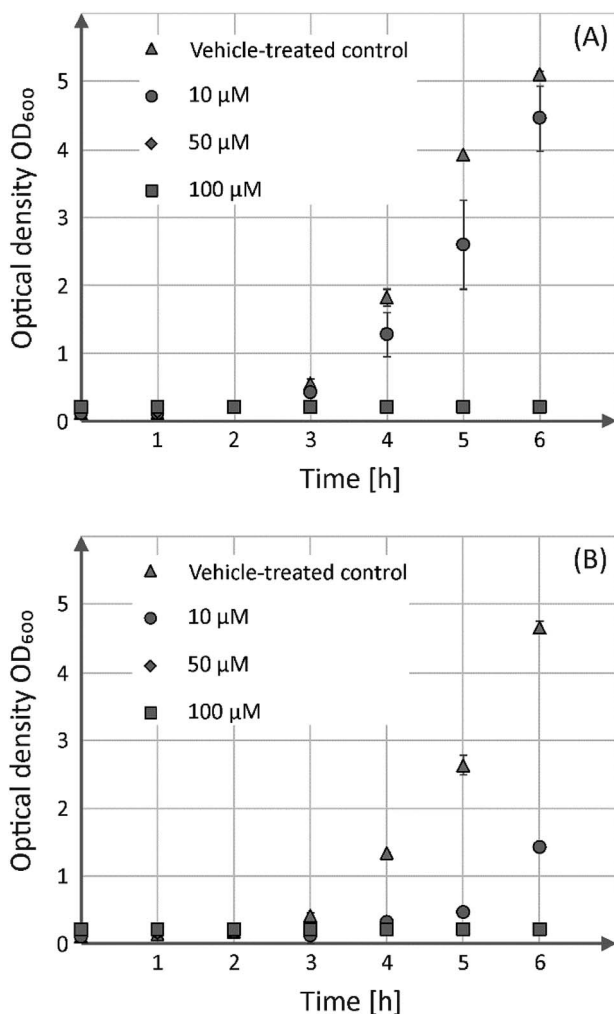

Fig. 4 Cell densities measured at a wavelength of 600 nm (OD$_{600}$) during cultivation of Gram-positive *B. subtilis* in the presence of 10 μM (circle), 50 μM (rhombus) or 100 μM (square) of S-1 (A) and R-1 (B), respectively.

These analyses showed that both enantiomers possess comparable growth inhibitory effects towards the Gram-positive strain, but have no bactericidal activity against its Gram-negative counterpart. Incubation of *B. subtilis* in the presence of 50 or 100 μM of either S-1 or R-1 prevents their growth entirely, whereas addition of 10 μM of both substances led only to growth delay.

Conclusions

We have developed a high yield synthetic route to chiral Schiff-base pocket ligands. A pair of chiral Schiff-base Cu(II)-clusters have been successfully prepared under aerobic conditions and these are the first examples of Cu(II) coordination clusters captured in chiral Schiff-base pocket ligands. Single-crystal X-ray analysis shows that S-1 and R-1 are isostructural and crystallize in the polar space group $P2_1$ with $Z = 2$. The crystallization in a polar space group highlights the efficient transfer of chirality from the chiral Schiff-base ligand to the coordination compound which exhibit the expected mirror image spectra for the Cotton effect using CD spectroscopy. Both enantiomerically pure Cu(II)-complexes exhibit anti-proliferative properties against human cell lines and anti-microbial activity against Gram-positive bacteria, although the observed effects of the complexes are independent of their chirality. Additionally, these Cu(II) chiral complexes will be further investigated as catalysts for asymmetric reactions. In addition we plan to study complexes formed with other M(II) ions.

Conflicts of interest

The authors declare no conflict of interest.

Acknowledgements

References

1 S. Dasari and P. B. Tchounwou, *Eur. J. Pharmacol.*, 2014, **740**, 364–378.

2 Y. Ho, S. C. F. Au-Yeung and K. K. W. To, *Med. Res. Rev.*, 2003, **23**, 633–655.

3 N. Graf and S. J. Lippard, *Adv. Drug Delivery Rev.*, 2012, **64**, 993–1004.

4 K. Yoh, K. Kubota, H. Ohmatsu, K. Goto, S. Niho and Y. Ohe, *Anticancer Res.*, 2012, **32**, 4131–4135.

5 N. P. E. Barry and P. J. Sadler, *Chem. Commun.*, 2013, **49**, 5106–5131.

6 G. F. Hu, *J. Cell. Biochem.*, 1998, **69**, 326–335.

7 C. K. Sen, S. Khanna, M. Venojarvi, P. Trikha, E. C. Ellison, T. K. Hunt and S. Roy, *Am. J. Physiol.: Heart Circ. Physiol.*, 2002, **282**, H1821–H1827.

8 C. J. M. D. Griffith and J. P. Parker, *Anti-Cancer Agents Med. Chem.*, 2010, **10**, 354–370.

9 C. Cox, T. N. Teknos, M. Barrios, G. J. Brewer, R. D. Dick and S. D. Merajver, *Laryngoscope*, 2001, **111**, 696–701.

10 J. Yoshii, H. Yoshiji, S. Kuriyama, Y. Ikenaka, R. Noguchi, H. Okuda, H. Tsujinoue, T. Nakatani, H. Kishida, D. Nakae, D. E. Gomez, M. S. De Lorenzo, A. M. Tejera and H. Fukui, *Int. J. Cancer*, 2001, **94**, 768–773.

11 Q. Pan, C. G. Kleer, K. L. van Golen, J. Irani, K. M. Bottema, C. Bias, M. de Carvalho, E. A. Mesri, D. M. Robins, R. D. Dick, G. J. Brewer and S. D. Merajver, *Cancer Res.*, 2002, **62**, 4854–4859.

12 L. Finney, S. Vogt, T. Fukai and D. Glesne, *Clin. Exp. Pharmacol. Physiol.*, 2009, **36**, 88–94.

13 X. Y. Qin, L. C. Yang, F. L. Le, Q. Q. Yu, D. D. Sun, Y. N. Liu and J. Liu, *Dalton Trans.*, 2013, **42**, 14681–14684.

14 A. E. Stacy, D. Palanimuthu, P. V. Bernhardt, D. S. Kalinowski, P. J. Jansson and D. R. Richardson, *J. Med. Chem.*, 2016, **59**, 4965–4984.

15 X.-Y. Qin, Y.-N. Wang, X.-P. Yang, J.-J. Liang, J.-L. Liu and Z.-H. Luo, *Dalton Trans.*, 2017, **46**, 16446–16454.

16 S. Zehra, T. Roisnel and F. Arjmand, *ACS Omega*, 2019, **4**, 7691–7705.

17 P. Daneshmand, J. L. Jime, M. Aragon–alberti and F. Schaper, *Organometallics*, 2018, **37**, 1751–1759.

18 C. M. Rajesh and M. Ray, *Dalton Trans.*, 2014, **43**, 12952–12960.

19 J. Pejic, D. Vušak, G. Szalontai, B. Prugovečki, D. Mrvoš-Sermek, D. Matković-Čalogović and J. Sabolovic, *Cryst. Growth Des.*, 2018, **18**, 5138–5154.

20 X. Zhou, Q. Sun, L. Jiang, S. Li, W. Gu, J. Tian, X. Liu and S. Yan, *Dalton Trans.*, 2015, **44**, 9516–9527.

21 M. Shibata, K. Nakajima and Y. Nishibayashi, *Chem. Commun.*, 2014, **50**, 7874–7877.

22 I. Castillo, V. Pérez, I. Monsalvo, P. Demare and I. Regla, *Inorg. Chem. Commun.*, 2013, **38**, 1–4.

23 M. J. MacLachlan, M. K. Park and L. K. Thompson, *Inorg. Chem.*, 1996, **35**, 5492–5499.

24 M. Andruh, *Dalton Trans.*, 2015, **44**, 16633–16653.

25 H. Yu, M. Liu, X. Gao and Z. Liu, *Polyhedron*, 2017, **137**, 217–221.

26 S. Karmakar and S. Khanra, *CrystEngComm*, 2014, **16**, 2371.

27 P. Adão, M. L. Kuznetsov, S. Barroso, A. M. Martins, F. Avecilla and J. C. Pessoa, *Inorg. Chem.*, 2012, **51**, 11430–11449.

28 M. Hazra, T. Dolai, A. Pandey, S. K. Dey and A. Patra, *J. Saudi Chem. Soc.*, 2017, **21**, S240–S247.